*Int. J. of Thermal & Environmental Engineering*
*Volume 6, No. 1 (2013) 7-14*

# Numerical Simulation of Force Convection in a Channel with Porous Part

**Mojtaba Aghajani Delavar*, Farzane Mohammadvali**

*Faculty of Mechanical Engineering, Babol Noshirvani University of Technology, Babol, Islamic Republic of Iran*

## Abstract

In the present work, two dimensional laminar flow and convective heat transfer between two parallel plates of a symmetric channel were simulated using Lattice Boltzmann Method (LBM). The channel was filled partially with a porous block. The Brinkman-Forchheimer model was used for porous zone. The effects of various parameters such as Reynolds number and porosity on the channel flow and thermal profiles were investigated. It was found that all these parameters have significant influence on thermal field of the channel in certain conditions.

***Keywords***: *Heat transfer, porosity, flow convection*

## 1. Introduction

Development of heat transfer in thermal devices such as heat exchangers and electronic equipment became an important issue in industry. For this reason, it is better to understand fundamental mechanisms in the fluid flow and thermal transport. The use of porous medium is one way for enhancing the heat transfer characteristics in industrial processes. This structure is used in many engineering applications such as thermal insulation, drying processes, geothermal systems and oil flow, as well as heat exchangers [1-6]. Many studies about porous medium have been investigated. Mukhopadhyay and Layek [5] analyzed the radiation effects on forced convective flow and heat transfer over a porous plate. It has been found that the Darcy's law is an important formula relating the pressure gradient, the viscous fluid resistance and the gravitational force for a forced convective flow in a porous medium. Bhargavi and Satyamurty [6] investigated three different structures of porous media in parallel plate channels subject to constant heat flux. It has been found that partial filling of porous medium in the central region causes the maximum enhancement in heat transfer. Alhajeri [7] presented a computational investigation of flow and heat transfer in a rectangular duct with ribs mounted in a staggered arrangement. It was found that the maximum values of the Nusselt numbers are located at a distance of almost one rib height ahead of the flow reattachment point. Anwarullah et al [8] investigated the effect of nozzle spacing on heat transfer and fluid flow characteristics of an impinging circular jet in cooling of electronic components. They found that for different Reynolds numbers, with reducing the jet diameter, surface temperature decreasing.

Recently Lattice Boltzmann Method (LBM) has been developed as a new method for simulating the fluid flow, heat transfer problems, thermal two-phase flow and other physical phenomena [9-16]. This is a micro and meso-scale modeling method based on the particle kinematics. Delavar Aghajani [9] investigated the effects of porous block and its location on heat transfer and entropy generation within a T-micromixer. It was shown that the porous block have important effects on mixing rate and flow pattern. Guo and Zhao [10] offered a Lattice Boltzmann Model for convective heat transfer by introducing a distribution function to simulate the temperature field. Kao et al. [11] investigated fluid flows through fixed-bed micro-reactors using Lattice Boltzmann Method and found that the optimal configuration and operating parameters to be established for the micro-reactor. Delavar Aghajani et al. [12] considered the effect of the heater location on flow pattern, heat transfer and entropy generation in a cavity by Lattice Boltzmann Method. The results showed that higher heat transfer was observed from the cold walls when the heater located on vertical wall. Peng et al. [13] investigated the simulation for incompressible flow in porous media by using LBM. In this work, it is intended to study the problem of forced convection in parallel-plate channel partially filled with single porous block using Brinkman-Forchheimer model. The effect of Reynolds number and porosity on the flow and thermal fields in the channel is investigated.

* Corresponding Author: Tel: +98-111-3234201,
Email: m.a.delavar@nit.ac.ir
© 2013 International Association for Sharing Knowledge and Sustainability
DOI: 10.5383/ijtee.06.01.002

### 2.1. LBE for Fluid Flow

Based on kinetic theory, the Lattice Boltzmann Method simulates fluid flows by using the single-particle density distribution. In this paper, the two-dimensional 9-speed lattice Boltzmann model (D2Q9) is used to solve the problem. The general form of Lattice Boltzmann equation is [12]:

(1)

Where $\Delta t$ denotes lattice time step, $f_k$ is the external force and $f_k^{eq}$ is the equilibrium distribution function. The flow properties in lattice model are defined as:

$$\rho = \sum_k f_k \ , \qquad \rho u_i = \sum_k f_k c_{ki} \tag{2}$$

### 2.2. LBE for Heat Transfer

As shown in section 2.1, the same procedure can be also applied to the Boltzmann energy equation. The resulting discrete scheme as the Lattice Boltzmann thermal equation describes the evolution of the macroscopic temperature field. The final discrete scheme is as [15,16]:

$$g_k\left(\vec{x}+\vec{c}_k\Delta t, t+\Delta t\right) = g_k\left(\vec{x},t\right) + \frac{\Delta t}{\tau_g}\left[g_k^{eq}\left(\vec{x},t\right) - g_k\left(\vec{x},t\right)\right]$$
$$g_k^{eq} = \omega_k . T . \left[1 + \frac{\vec{c}_k.\vec{u}}{c_s^2}\right], \quad T = \sum_k g_k \tag{3}$$

For simulating porous media the Brinkman-Forchheimer equation has been applied. This final equation as considered below was used for both fluid and porous zones [18]:

$$\frac{\partial \vec{u}}{\partial t} + \left(\vec{u}.\nabla\right)\left(\frac{\vec{u}}{\varepsilon}\right) = -\frac{1}{\rho}\nabla\left(\varepsilon p\right) + \upsilon_{eff}\nabla^2\vec{u} + \kappa\left(-\frac{\varepsilon\upsilon\vec{u}}{K} - \frac{1.75\left|\vec{u}\right|\vec{u}}{\sqrt{150\varepsilon K}}\right)$$

$$\kappa = \begin{cases} 0, \varepsilon = 1 \\ 1, \varepsilon \neq 1 \end{cases} \tag{4}$$

For porous medium the equilibrium distribution functions and the suitable forcing term, $F_k$, used in Eq. (1) is taking [17]:

$$f_k^{eq} = \omega_k . \rho . \left[1 + \frac{\vec{c}_k.\vec{u}}{c_s^2} + \frac{1}{2}\frac{\left(\vec{c}_k.\vec{u}\right)^2}{\varepsilon c_s^4} - \frac{1}{2}\frac{\vec{u}^2}{\varepsilon c_s^2}\right]$$
$$F_k = \omega_k \rho \left(1 - \frac{1}{2\tau_\upsilon}\right)\left[\frac{\vec{c}_k.\vec{F}}{c_s^2} + \frac{\left(\vec{u}\vec{F} : \vec{c}_k\vec{c}_k\right)}{\varepsilon c_s^4} - \frac{\vec{u}.\vec{F}}{\varepsilon c_s^2}\right] \tag{5}$$

For improving the conduction and convection heat transfer in porous medium, the effective thermal conductivity ( $k_{eff}$ ) should be determined which was calculated by [17]:

$$k_{eff} = k_f\left[\left(1-\sqrt{1-\varepsilon}\right) + \frac{2\sqrt{1-\varepsilon}}{1-\sigma B}\left(\frac{(1-\sigma)B}{(1-\sigma B)^2}\ln\left(\frac{1}{\sigma B}\right) - \frac{B+1}{2} - \frac{B-1}{1-\sigma B}\right)\right]$$

$$\sigma = k_f / k_s, \quad B = 1.25\left[(1-\varepsilon)/\varepsilon\right]^{10/9} \tag{6}$$

Which $k_f$ and $k_s$ are fluid and solid thermal conductivities.

## 3. Boundary Condition

To determine the unknown distribution functions which are out of the solution domain, the streaming process is used. For solid boundaries the bounce back scheme is applied as a result of no slip condition. For example for top adiabatic wall, the boundary condition is defined as below:

$$f_{4,n} = f_{2,n} \quad f_{8,n} = f_{6,n} \quad f_{7,n} = f_{5,n} \tag{7}$$

$$g_{4,n-1} = g_{4,n} \quad g_{7,n-1} = g_{7,n} \quad g_{8,n-1} = g_{8,n} \tag{8}$$

## 4. Computational Domain and Validation

A schematic of the physical model for a porous/fluid composite system is shown in Fig.1. This figure displays a two dimensional incompressible flow through the channel that is partially filled with a porous block. It is assumed that the flow is steady, Newtonian and laminar. The porous medium is considered to be homogeneous, isotropic, and in local thermodynamic equilibrium with saturated fluid. For all simulation, 50000 iterations are sufficient to get converged solution for a $450\times50$ grid. This grid was selected after a grid check between 270×30, 360×40, 450×50 and 60×540 grid sizes. No sensible difference was observed between two last grids, due to CPU time saving the grid 450×50 was selected. To validate this model, the result compares well velocity profiles in clear and porous regions fluid interface in LB model with Alazmi and Vafai [19], Fig 2. ( $T^* = \frac{T - T_{in}}{T_w - T_{in}}$ ).

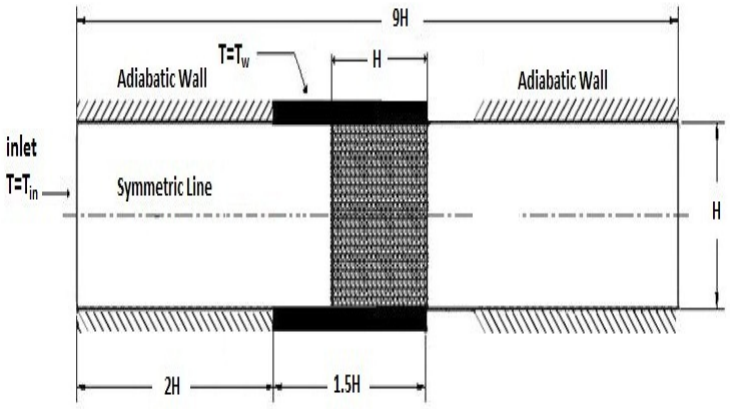


**Fig.1. Schematic illustration of the problem under consideration**

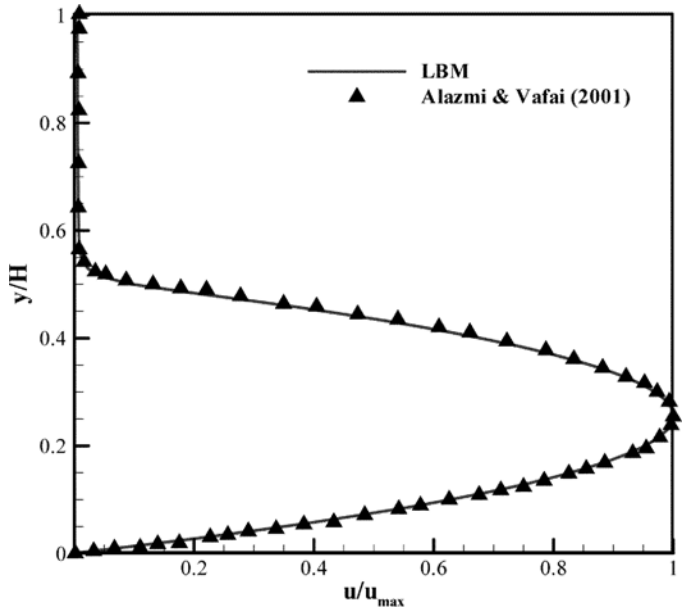


**Fig.2. Comparison of velocity profile in channel partially filled with porous media.**

$n$ indicates the lattice on the boundary and $n-1$ is the lattice near the boundary within the solution domain. For boundaries with specified temperature, $T = T_{in}$, the unknown distribution function is:

$$\begin{aligned} g_{1,n} &= T_{in}\left(\omega_1 + \omega_3\right) - g_{3,n} \\ g_{5,n} &= T_{in}\left(\omega_5 + \omega_7\right) - g_{7,n} \\ g_{8,n} &= T_{in}\left(\omega_8 + \omega_6\right) - g_{6,n} \end{aligned} \tag{9}$$

## 5. Result and discussion

in this work the effects of Reynolds number and porosity on the channel flow and thermal profiles were investigated. It is believed that the presence of porous block can change the characteristics of flow and thermal field significantly.

Figure 3 shows the dimensionless temperature ( $T^*$ ) for different Reynolds numbers. It is shown that with increasing Reynolds number from 30 to 90, the fluid velocity increases, the convective coefficient (h) increased and the heat transfer increases ( $(Q = hA_c(T_w - T_{fluid}))$ . But with increasing Reynolds number, according to $(Q = \dot{m}C\Delta T = \rho u A_c(T_{out} - T_{in}))$ decreases the temperature of fluid flow. The results show that the reduction of temperature difference of fluid flow is dominant and the temperature reduces about 40% at $\mathrm{Re} = 90$ .

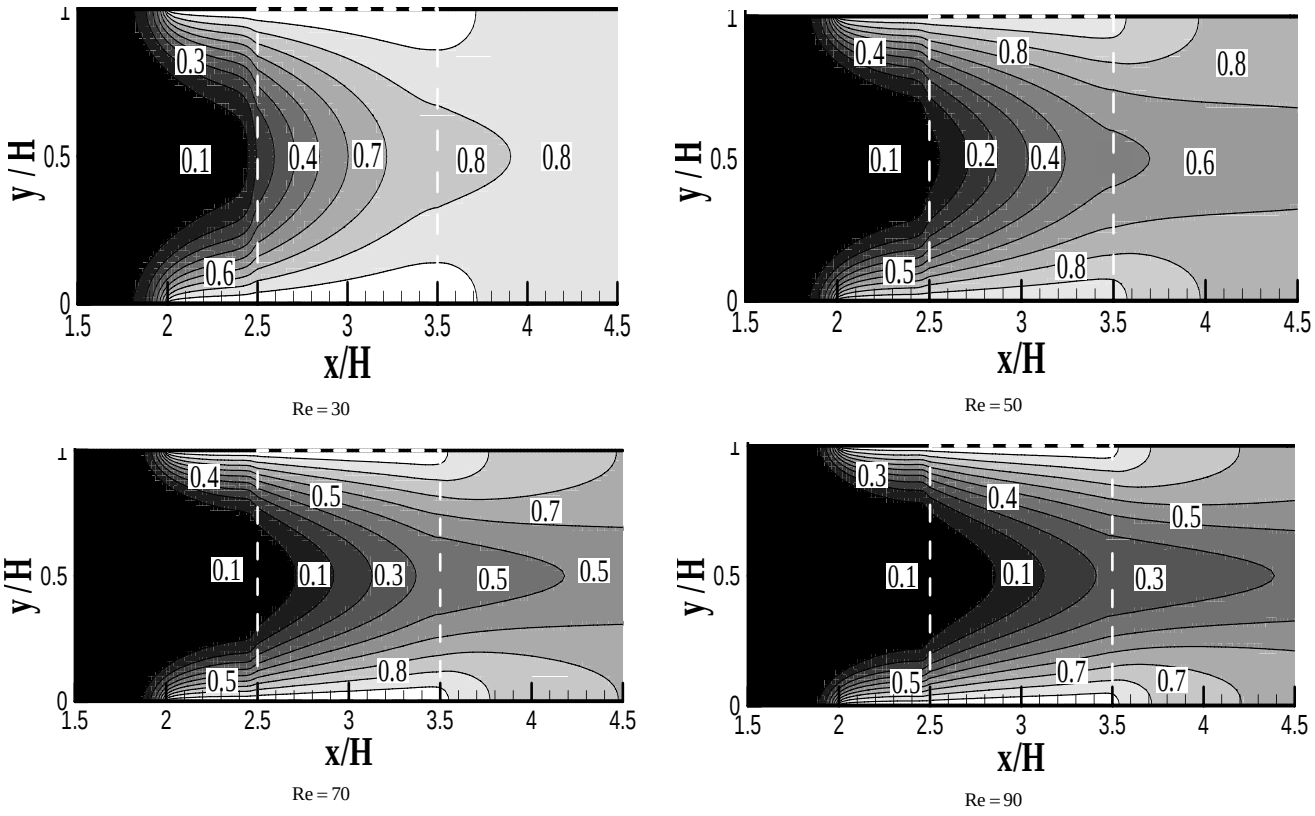


**Fig. 3. Normalized temperature ( $T^*$ ) contours in the channel for different Reynolds numbers for** $Da = 1\times10^{-2}$ , $\varepsilon = 0.7$ , $\sigma$=$10^{-3}$.

The dimensionless temperature ($T^*$) for different porosities is illustrated in Fig. 4. For the case of a lower block porosity, $\varepsilon = 0.3$ , because of the larger effective conductivity (Eq.8), the heat transfer from the block to fluid flow enhances and it is greater approximately 40% than higher block porosity, $\varepsilon = 0.9$ , thus the heat conduction plays an important role at low block porosity. Furthermore, with increasing porosity, the temperature distribution in porous block becomes more uniform.

Figure 5 shows the normalized velocity contours $\left(u/u_{\max-\mathrm{Re}=30}\right)$ for different Reynolds numbers. It is found that for specific block porosity, with increasing Reynolds number, because of the more effect of flow convection, the velocity increases in porous block and non-porous region. And for lower Reynolds number the velocity distribution has no significant changes between porous block and clear channel and it is more uniform for lower Reynolds number.

Figure 6 shows that for a specific Reynolds number, it is easier for fluid to pass the clear channel at higher porosity. It is obvious the average velocity for different porosities is the same, but changing the boundary layer within the porous region changes the maximum velocity at different cases.

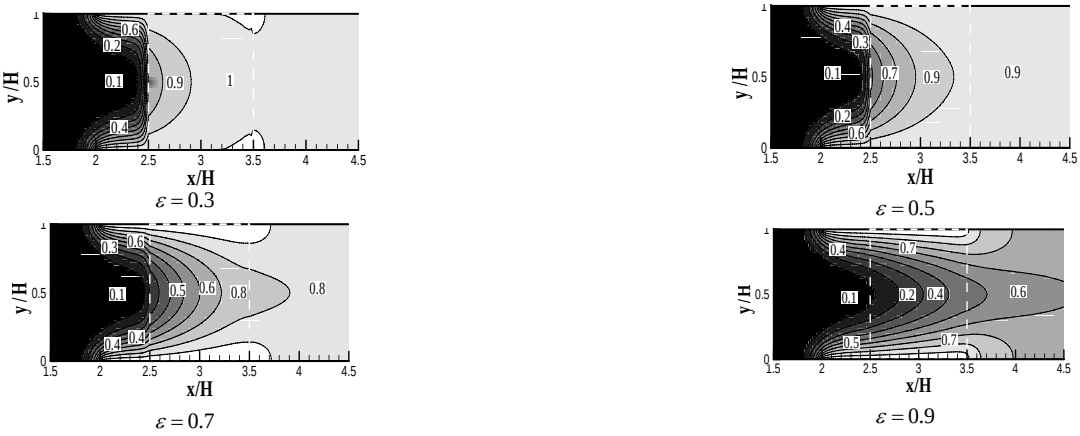


**Fig. 4. Normalized temperature ( $T^*$ ) contours in the channel for different porosities for** $Da = 1\times10^{-2}$ **,** $\mathrm{Re} = 30$ **,** $\sigma$=$10^{-3}$ **.**

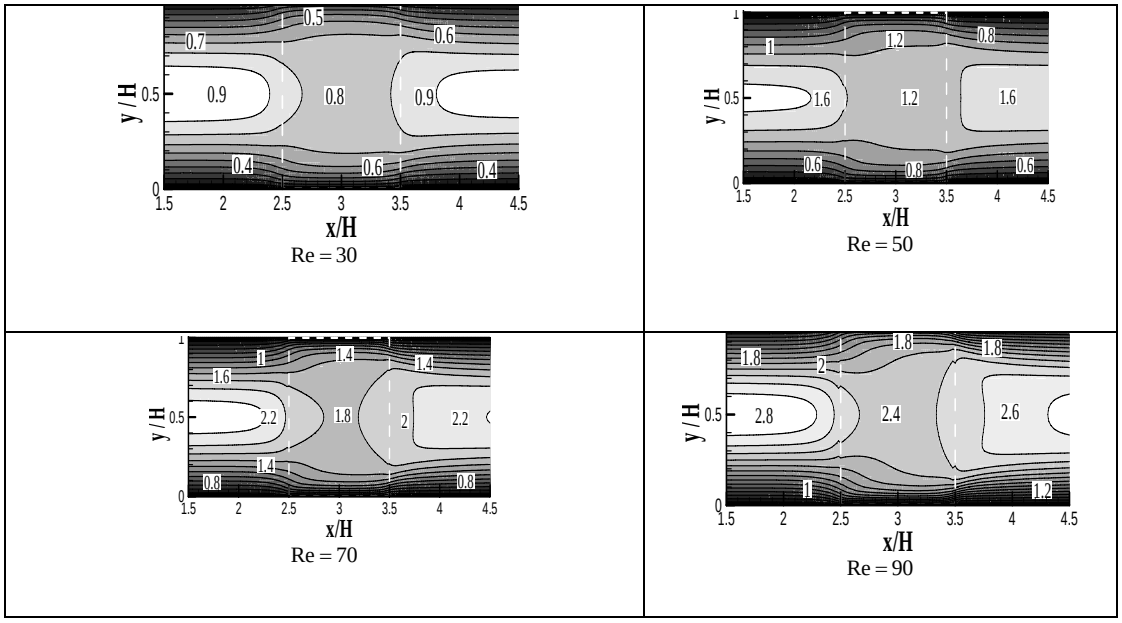


**Fig. 5. Normalized velocity $\left(u/u_{\max-\mathrm{Re}=30}\right)$ contours in the channel for different Reynolds numbers for $Da=1\times10^{-2}$, $\varepsilon=0.7$, $\sigma=10^{-3}$.**

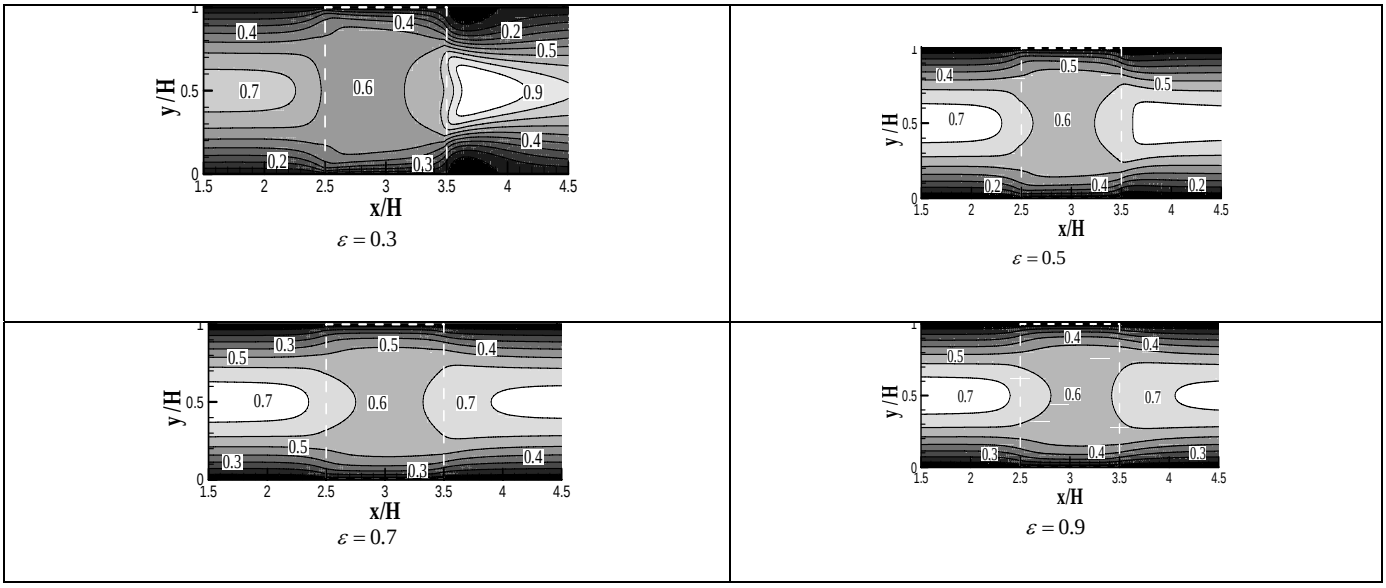


**Fig. 6. Normalized velocity $\left(u/u_{\max-\varepsilon=0.3}\right)$ contours in the channel for different porosities for, $Da=1\times10^{-2}$, $\mathrm{Re}=30$, $\sigma=10^{-3}$.**

For $\varepsilon=0.3$, with starting the porous block, the boundary layer grows up and the block acts like an thin obstacle near the walls and the fluid velocity is zero in this regions. After block the velocity increases and fluid flow moves in clear channel easier, and it causes to form vortex at lower porosity.

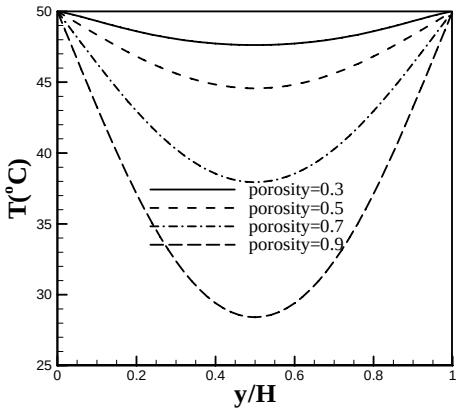


a

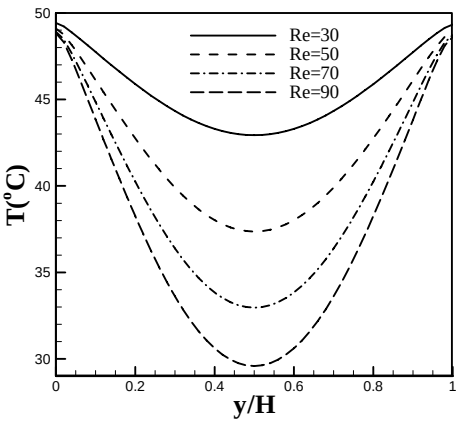


b

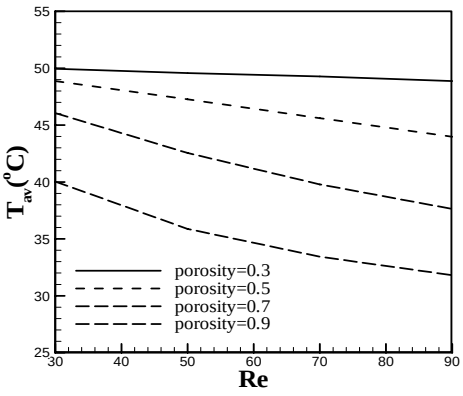


c

**Fig. 7.a) Effect of block porosity on the temperature, for** $Da = 1\times10^{-2}$ **,** $\mathrm{Re} = 30$ **,** $\sigma$=$10^{-3}$ **at** $x = 3H$ **, b) Effect of Reynolds number on the temperature.** $Da = 1\times10^{-2}$ **,** $\varepsilon = 0.7$ **,** $\sigma$=$10^{-3}$ **at** $x = 3H$ **, c) Effect of Reynolds number on the average temperature for different porosities after porous block at** $x = 3.5H$ **.**

The temperature profile at $x = 3H$ for different porosities is illustrated in Fig. 7a. As porosity decreases, the temperature profile becomes more uniform. According to (Eq. (8)), for lower porosity $\varepsilon = 0.3$ , because of larger effective conductivity, the heat transfer from block to fluid flow increases so the magnitude of temperature become greater than higher porosity $\varepsilon = 0.9$ . The result shows that the block with higher porosity increases the flow convection effect and reduces the thermal diffusion inside porous block. From Fig. 7b, it is found that for lower Reynolds numbers, the temperature has larger values, and has more uniform profile. Because with increasing Reynolds number and velocity the flow convection effect increases, the heat transfer rate from the wall to fluid flow increases but the temperature difference of flow, $\Delta T$ , decreases, because the fluid has less time to get heat from the wall. So the temperature decreases for higher Reynolds number. As shown in Fig. 7c, with increasing Reynolds number, the average temperature after porous block, $x = 3.5H$ , decreases. For lower block porosity, the heat diffusion (conduction) is dominant because of larger effective conductivity and it causes the increase of temperature compared with higher porosity (more effect of flow convection), and so increasing Reynolds number has no significant changes on temperature for $\varepsilon = 0.3$ .

Figure 8a shows the effect of Reynolds number on local Nusselt number at upper constant temperature wall. It is shown that the Nusselt number increases with increasing Reynolds number. Larger Reynolds number, causes the larger wall shear stress at solid walls and the interface between porous block and fluid region, thus the temperature gradients increase which result in heat transfer rate and larger Nusselt number. The result of Fig.8b shows that the average Nusselt number at upper wall has larger values for higher Reynolds number at certain porosity, and for higher porosity, the average Nusselt number increases.

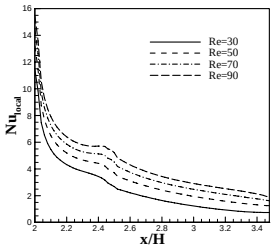


a

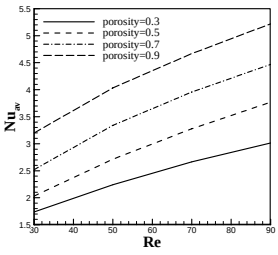


b

**Fig. 8.a) Effect of Reynolds number on the local Nusselt number, for** $Da = 1\times10^{-2}$ **,** $\varepsilon = 0.7$ **,** $\sigma$=$10^{-3}$ $x = 2.5H$ **, b) Effect of Reynolds number on the average Nusselt number for different porosity,** $Da = 1\times10^{-2}$ **,** $\sigma$=$10^{-3}$ **at porous block location.**

The vertical velocity profiles at $x = 3H$ inside the block is shown in Fig. 9a. It is inferred that for different porosities, the average velocity is nearly the same for a constant Reynolds number, but at boundary layer because of the flow convection, the maximum velocity differs for different cases and for higher porosity the maximum fluid velocity increases. Fig. 9b, displays that with increasing Reynolds number the average velocity increases and near the wall because of the flow convection in boundary layer, the vertical velocity profile changes. For lower Reynolds number, the velocity profile is more uniform.

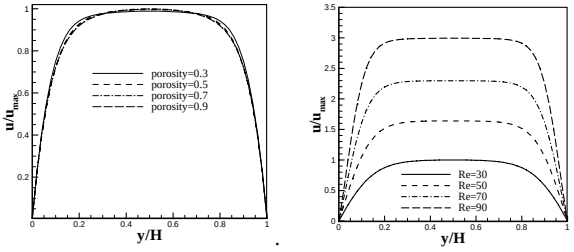


a b

**Fig. 9.a) Effect of the porosity on the normalized, for** $Da = 1\times10^{-2}$ , $\mathrm{Re} = 30$ , $\sigma$=$10^{-3}$ **at** $x = 3H$ **, b) Effect of the Reynolds number on the normalized velocity for** $Da = 1\times10^{-2}$ , $\varepsilon = 0.7$ , $\sigma$=$10^{-3}$ **at** $x = 3H$ **.**

## 6. Conclusion

A Lattice Boltzmann Method (LBM) for numerical simulation of two dimensional, incompressible, laminar flow and forced convection heat transfer in a channel has been presented. The effects of various parameters such as Reynolds number and porosity was considered. It was found that the porous media has significant influence on heat transfer and flow characteristic. It is found that increasing Reynolds number decreases the temperature inside the porous block. At lower porosity of porous block because of larger effective conductivity, the heat conduction is dominant than higher porosity. The investigation shows that the Nusselt number increases with increasing Reynolds number because of the larger shear stress as result of increasing temperature gradients at solid wall. For different porosities the average velocity is nearly the same for a specific Reynolds number, but the boundary layer near the wall changes the maximum velocity for each cases.

## Nomenclature

| | | |
|---|---|---|
| $A$ | : | Area, $m^2$ |
| $C$ | : | Specific heat capacity, kJ/kg.K |
| $c$ | : | discrete lattice velocity |
| $Da$ | : | Darcy number ( $KH^{-2}$ ) |
| $F$ | : | external force |
| $f$ | : | distribution function for flow |
| $g$ | : | distribution function for temperature |
| $H$ | : | characteristic Height, m |
| $K$ | : | Permeability |
| $k$ | : | thermal conductivity, $W/m^2.K$ |
| $p$ | : | Pressure, Pa |
| $T$ | : | Temperature, K |
| $t$ | : | time, s |
| $u$ | : | velocity component in x direction, m/s |
| $v$ | : | velocity component in y direction, m/s |
| $x$ | : | axial coordinate |

*Greek Symbols*

| | | |
|---|---|---|
| $\varepsilon$ | : | is the porosity of porous media |
| $\upsilon$ | : | kinematic viscosity, $m^2/s$ |
| $\rho$ | : | Density, $kg/m^3$ |
| $\tau$ | : | relaxation time |
| $\mu$ | : | Dynamic viscosity, Pa.s |

*Superscripts*

| | | |
|---|---|---|
| *eq* | : | equilibrium distribution function |

*Subscript*

| | | |
|---|---|---|
| *c* | : | Cross section |
| *eff* | : | Effective |
| *fluid* | : | Fluid |
| *i* | : | dimension direction |
| *in* | : | Inlet |
| *k* | : | lattice model direction |
| *out* | : | Outlet |
| *s* | : | Sound – solid |
| *w* | : | Wall |
| $\omega$ | : | weighting factor |

*Non-dimensional Numbers*

| | | |
|---|---|---|
| Re | : | Reynolds number |

### References

[1] C. Y. Cheng. Natural convection heat transfer of non-Newtonian fluids in porous media from a vertical cone under mixed thermal boundary conditions. Int. J. Heat & Mass Transfer 2010; 36: 693-697.

[2] C. Yang, W. Liu, A. Nakayama. Forced convective heat transfer enhancement in a tube with its core partially filled with a porous medium. J. The Open Transport Phenomena Journal 2009; 1:1–6.

[3] N. B. Santos, M. J . S. D. Lemos. Flow and heat transfer in a parallel-plate channel with porous and solid baffles. J. Numerical Heat Transfer 2006; 49: 471-494.

[4] P. C. Huang, C. F. Yang, J. J. Hwang, M. T. Chiu. Enhancement of forced-convection cooling of multiple heated blocks in a channel using porous covers. Int. J. Heat & Mass Transfer 2005; 48: 647-664.

[5] S. Mukhopadhyay, G. C. Layek. Radiation effect on forced convective flow and heat transfer over a porous plate in a porous medium. J. Meccanica 2009; 44: 587-597.

[6] D. Bhargavi, V. V. Satyamurty. Optimum porous insert configurations for enhanced heat transfer in channels. J. Porous Media 2011; 10: 187-203.

[7] M. Alhajeri. Computational Investigation of Flow and Heat Transfer in a Rectangular Duct with Ribs Mounted in a Staggered Arrangement. Int. J. of Thermal & Environmental Engineering 2012; 1: 81-88.

[8] M. Anwarullah, V. Vasudeva, Rao K.V. Sharma. Effect of Nozzle Spacing on Heat Transfer and

Fluid Flow Characteristics of an Impinging Circular Jet in Cooling of Electronic Components. Int. J. of Thermal & Environmental Engineering 2012; 1: 7-12.

[9] M. A. Delavar. Engineering using lattice Boltzmann method to investigate the flow and entropy generation inside a T-micromixer with a porous block. J. ASME proceeding of International Conference on Physics Science and Technology 2011; 55-57.

[10] Z. Guo, T. S. Zhao. A lattice Boltzmann model for convection heat transfer in porous media. J. Numerical Heat Transfer, Fundamentals 2005; 47: 157-177.

[11] P. H. Kao, T. F. Ren, R. J. Yang. An investigation into fixed-bed microreactors using lattice Boltzmann method simulations. Int. J. Heat & Mass Transfer 2007; 50: 4243-4255.

[12] M. A. Delavar, M. Farhadi, K. Sedighi. Effect of the heater location on heat transfer and entropy generation in the cavity using the lattice Boltzmann method. J. Heat Transfer Research 2009; 40: 521-536.

[13] Y. Peng, C. Shu, Y. T. Chew. Simplified thermal lattice Boltzmann model for incompressible thermal flows. J. Physical Review 2003; 68: 026701.

[14] A. A. Mohammad. Lattice Boltzmann Method Fundamentals and Engineering Applications with Computer Codes. J. Springer-Verlag 2011.

[15] X. Y. He, S. Y. Chen, G. D. Doolen. A novel thermal model for the lattice Boltzmann method in incompressible limit. J. Computational Physics 1998; 146: 282-300.

[16] J. K. Wang, M. R. Wang, Z. X. Li. A lattice Boltzmann algorithm for fluid–solid conjugate heat transfer, Int. J. Thermal Sciences 2007; 46: 228-234.

[17] J. Peixue, X. C. Lu. Numerical simulation of fluid flow and convection heat transfer in sintered porous plate channels. Int. J. Heat & Mass Transfer 2006; 49: 1685-1695.

[18] S. Takeshi, T. Eishun, K. Kazuyuki, O. Kenichi. Thermal Lattice Boltzmann Model for Incompressible Flows through Porous Media. Int. J. Thermal Science & Technology 2006; 1: 90-100.

[19] B. Alazmi, K. Vafai. Analysis of fluid flow and heat transfer interfacial conditions between a porous medium and a fluid layer. Int. J. Heat & Mass Transfer 2001; 44: 1735-1749.